Clim. Past Discuss., 8, 4701–4744, 2012
www.clim-past-discuss.net/8/4701/2012/
doi:10.5194/cpd-8-4701-2012

Climate of the Past Discussions

Orbital changes, variation in solar activity and increased anthropogenic activities: controls on the Holocene flood frequency in the Lake Ledro area, Northern Italy

B. Vannière[1], M. Magny[1], S. Joannin[1,2], A. Simonneau[3], S. B. Wirth[4], Y. Hamann[4], E. Chapron[3], A. Gilli[4], M. Desmet[5], and F. S. Anselmetti[6]

[1]CNRS, UMR6249, Besançon, France
[2]LGL TPE, Université Lyon 1, Villeurbanne, France
[3]ISTO, UMR7327, Orléans, France
[4]Geological Institute, ETH Zurich, Switzerland
[5]GEHCO, University of Tours, France
[6]Geological Institute, University of Bern, Switzerland

Received: 4 September 2012 – Accepted: 10 September 2012
– Published: 24 September 2012

Correspondence to: B. Vannière (boris.vanniere@univ-fcomte.fr)

Published by Copernicus Publications on behalf of the European Geosciences Union.

Abstract

Two lacustrine sediment cores from Lake Ledro in Northern Italy were studied to produce chronologies of flood events for the past 10 000 yr. For this purpose, we have developed an automatic method that objectively identifies the sedimentary imprint of river floods in the downstream lake basin. The automatic counting of flood deposits was based on colour data extracted from processed core photographs, and the count data were processed to capture the flood signal. Automatic quantification was compared with naked-eye counting. Counts were performed twice on the proximal and distal cores to provide an objective and reproducible record of flood frequency. Geophysical and geochemical analyses made it possible to distinguish event deposits from background sedimentation. Flood frequency and reconstructed sedimentary dynamics were compared with lake-level changes and pollen dynamics inferred from vegetation data. The data suggest a record marked by low flood frequency during the early and middle Holocene (10 000–4500 cal BP). Only modest increases during short intervals are recorded at ca. 8000, 7500, and 7100 cal BP. The last third of the Holocene is characterised by a shift toward increased flood frequency at ca. 4500–4000 cal BP. With the exception of two short intervals around 2900–2500 and 1800–1400 cal BP, which show a slightly reduced number of floods, the trend of increasing flood frequency prevailed until the 20th century, reaching a maximum between the 16th and the 19th centuries. Brief-flood frequency increases recorded during the early and middle Holocene can be attributed to cold climatic oscillations. On a centennial time scale, major changes in flood frequency, such as those observed at ca. 4500 and 500 cal BP, can be attributed to large-scale climatic changes such as the Neo-glacial and Little Ice Age, which are under orbital and possibly solar control. The role of climate as the main forcing factor in flood activity is supported by the lake-level records: the major lake-level rises are synchronous with flood frequency increases. However, in the Bronze Age and during the Middle Ages and modern times, forest clearing and land use are indicated by pollen and archaeological data. These human activities have clearly affected the sediment

record of flood activity, and they can partially explain the amplitude of the increases in flood activity.

1 Introduction

Understanding the respective roles of climate and land-use change on long-term ecosystem dynamics have become an important issue of palaeo-studies (Dearing et al., 2006; Hoffmann et al., 2010), particularly since the Ruddiman's hypothesis about the anthropogenic greenhouse era (2003, 2007). One of the main questions addresses the tipping elements that indicate ecosystems dynamics (Lenton et al., 2008) over the Holocene controlled by climatic or human forcing factors (Magny et al., 2009; Hoffmann et al., 2008). For instance, at the end of the Holocene Thermal Maximum ca. 5000 yr ago (Renssen et al., 2009), Southern European ecosystems experienced great changes, as observed in glacier dynamics (Matthew et al., 2008), lake-levels (Magny et al., 2011), fire activity (Vannière et al., 2011) and flood records (Macklin and Lewin, 2003). In contrast to this period, the Bronze Age (4200–2800 cal BP) in Italy and across Europe was a crucial period for societal development, involving important technological innovations and changes in land-use strategies (Valsecchi et al., 2006; Vannière et al., 2010; Zolitschka et al., 2003).

River floods are among the most common and widespread natural disasters, and there is a societal debate about whether the frequency of such flood events varies due to changes in human land-use and/ or anthropogenic climate change (Coulthard and Macklin, 2001; Chapron et al., 2005; Moreno et al., 2008). Several climate scenarios may trigger flood events. Flood chronologies from several regions suggest that times of rapid climate changes are associated with a greater frequency of large and extreme floods (Macklin et al., 2006; Vasskog et al., 2011). Records of palaeofloods show that natural floods resulting from excessive rainfall, snowmelt, or both combined are highly sensitive to even modest changes of climate (Knox, 2000). Land use and human-driven land cover changes are also considered important forcing/controlling factors of flood activity and global sediment flux (Macklin and Lewin, 2003; Dearing and Jones, 2003).

Lakes provide valuable records of environmental changes because they are such sensitive ecosystems (Battarbee and Bennion, 2011), but also because their sediment accumulations offer exceptionally high-resolution, continuous terrestrial archives of past changes and a long-term perspective on ecosystem trajectories (Dearing et al., 2006). Lake sedimentation is very good at preserving river-flood activity at the event scale and offers continuous records of sedimentary flood deposits, which enables the estimation of long-term event frequency (Gilli et al., 2012; Støren et al., 2010; Wilhelm et al., 2012).

This paper presents a lacustrine approach to establish a Holocene flood record in Southern Europe. This flood dataset is based on the chronological occurrence of detrital deposits in the sediment record of the perialpine Lake Ledro (Alps, Northern Italy). Two sediment cores were studied, and an automatic method was developed that objectively identifies the sedimentary imprint of river floods in the downstream lake basin. The automatic quantification was made twice on the proximal and the distal cores to produce a reproducible record of flood frequency. Geophysical and geochemical analyses made it possible to distinguish event deposits (flood and mass-wasting events) from background sedimentation. The reconstruction of flood frequency was compared with (1) lake-level changes, which respond to longer-term variations in the hydrological regime, and (2) land-cover changes from pollen data, which also document land-use history. The principal objective of this paper is to highlight the main shift of Holocene ecosystem dynamics and to discuss the magnitude of such changes in the context of climatic versus human forcing factors.

CPD
8, 4701–4744, 2012

2 Materials and methods

2.1 Study site

Lake Ledro (45° 52′ N, 10° 45′ E, 652 m a.s.l.), located on the southern slope of the Alps in Italy, is a small lake (3.7 km^2) with a maximum depth of 46 m (Fig. 1). The catchment area covers 111 km^2 and includes several mountains that culminate between 1500 and 2250 m a.s.l. Two tributaries feed the lake: the Massangla and the Pur rivers. The lake was dammed by a moraine (Beug, 1964) that was partially cut by the outflowing Ponale River, which flows into nearby Lake Garda (65 m a.s.l.). Triassic, Liassic and Cretaceous limestone mainly constitutes the geological substratum. Some morainic tongues and alluvial deposits of calcareous and siliceous composition fill the bottom of the valleys. Lake sediments are dominated by autochthonous carbonate lake-marl that forms a rim of white platform along the shore. The vegetation around the lake is dominated by *Fagus* mixed with *Abies*. Higher in the Ledro Valley, between 650–1600 m a.s.l., the forest is dominated by *Picea*. Above 1600 m, grassland replaces forest. At Lake Ledro, the modern climate conditions can be considered sub-continental. The coldest and the warmest months have average temperatures of 0 °C and 20 °C, respectively. The annual precipitation ranges ~ 750 to 1000 mm.

On the River Ponale, between Lake Ledro and Lake Garda, the pumped-storage plant "Centrale idroelettrica del Ponale" was built in 1928–1929. Water is pumped in penstocks from Lake Garda to Lake Ledro, which is 532 m higher. This artificial water regulation strongly modifies the sedimentary dynamics. Consequently, the sedimentary record since 1929 cannot be compared to the older parts of the record or used as a reference. During construction of the pumped-storage plant, the remains of a Bronze Age pile-dwelling village (over 10 000 piles) were discovered on the eastern shore of the Lake. Lake settlements started around 4000–3800 cal BP and ended with abandonment between 3200–2800 cal BP (Pinton and Carrara, 2007).

2.2 Seismic survey and coring

A seismic reflection survey using a single-channel 3.5 kHz pinger source provided the lake bathymetry and high-resolution sub-bottom profiles used to establish a seismic stratigraphy of the well preserved part of the basin infilling (Fig. 1; Simonneau et al., 2012). Cores LL08-1 and LL08-2 were located in the deep basin within a well stratified seismic facies highlighting continuous and high-frequency reflections, i.e. by avoiding chaotic and larger mass-wasting deposits (MWD). Core LL08-1 is in a relatively distal position from the two main deltas constructed by the lake tributaries, whereas core LL08-2 is more proximal to the inflow of allochthonous particles. The sediment-water interface was properly recovered by using a gravity corer equipped with ⌀ 63 mm PVC liners. Sediment cores were retrieved using a piston corer with the same liners (UWITEC system). Duplicate cores were taken from each site (LL08-1 and LL08-2).

2.3 Geophysics logging

Magnetic susceptibility (MS) and Gamma-ray attenuation bulk density (GD) were measured in the cores at 5 mm resolution with a Geotek multi-sensor core logger (Gunn and Best, 1998). GD was logged on whole cores and MS was measured on split cores with the MS2E1 surface-scanning sensor from Bartington Instruments, which was adapted for fine-resolution volume magnetic-susceptibility measurements (Vannière et al., 2004). These analyses allow us to establish stratigraphic correlations useful for constructing the master sequences (LL08-1 and LL08-2), guaranteeing complete records without any gaps or redundancies. Colour properties were analysed with a line scan camera with 3 CCDs (2048 pixels each). Colour data are reported in the RGB and Lab-colour systems at a resolution of 70 µm, providing a continuous record of the master sequences at very high resolution.

CPD
8, 4701–4744, 2012

2.4 Geochemical analysis

The chemical composition of sediment core LL08-1 was analysed using an Avaatech XRF core scanner at a resolution of 0.2 mm (presented here: Si, Ca, K, Ti) and 2 mm (Zr). The XRF measurements were carried out on split cores with a measurement duration of 20 s. A 10 kV voltage and a 2000 µ A current were applied to detect lighter elements (Si, Ca, K, Ti), and 30 kV and 1000 µA settings were used for the heavier elements (Zr). Because of the influences of variable water content and grain size on the sediment matrix, the XRF scanner only provides a rough estimate of the geochemical composition, and the acquired counts are semi-quantitative. The Ca, Si, K, Ti and Zr results are presented for a short section to complete the lithological characterisation (Fig. 2b). To calibrate the XRF measurements and to analyse selected layers, 49 samples from the laminated facies of LL08-1 were processed for inductively coupled plasma-atomic emission spectrometry (ICP-AES) measurements. Approximately 80 mg of sediment were fully dissolved under pressure at 100 °C using a mixture of 2 ml each of suprapure grade HCl, HNO_3 and HF. After evaporation, the residues were mixed again with HNO_3 and diluted with MilliQ water. Certified reference materials (BCSS1, JSD1, PACS1 and BCR2), 5 "white samples" (i.e. lacking sediment), and 5 duplicates were added to the set of samples. Only Zr and Ca elemental concentrations (ppm) are presented.

2.5 Organic matter characterisation

Twelve samples were taken from unlaminated brown and light grey deposits of LL08-1 for organic matter petrographic observations. Petrographic study (palynofacies) involves microscopic examination of total OM in transmitted and reflected light after acid hydrolysis of carbonates and silicates. Taking into account the chromatic and textural aspects of particles (Meyers and Lallier-Vergès, 1999), the analysis aims to identify and quantify the organic compounds (relative percentages of surface particle area) and establish the ratio between allochthonous and autochthonous components. Terrestrial

CPD
8, 4701–4744, 2012

OM (TOM) includes particles weathered from the catchment and/or windblown grains, while lacustrine OM (LOM) consists of particles derived from aquatic plants and phytoplankton (Millet et al., 2007).

2.6 Pollen analyses

For pollen analyses, the mean sampling resolution ($1\,cm^3$ and 1 cm thickness) on the whole LL08-1 sequence is 5 cm. Samples were taken from laminated parts of the series. Samples were treated chemically (HCl, KOH, HF, acetolysis) and physically (0.5 mm sieving and decanting) following standard procedures (Moore et al., 1991). Lycopodium markers (Stockmaar, 1971) were added to estimate pollen concentrations (grains cm^{-3}). For the identification of pollen types, we used keys (Beug, 2004; Reille, 1992–1998) as well as the reference collection at the University of Franche-Comté. At least 300 terrestrial pollen grains were counted in total, excluding dominant terrestrial taxa, water and wetland plants, as well as spores of pteridophytes. This paper presents only arboreal and non-arboreal pollen (AP/NAP) curves and an "anthropic" pollen-sum curve (Cerealia type, Secale type, Triticum type, Cannabis-humulus type, *Plantago lanceolata*, *Rumex*, *Urticaceae*). A related paper (Joannin et al., 2012) is dedicated to the reconstruction of detailed vegetation dynamics around Lake Ledro.

2.7 ^{14}C and ^{137}Cs measurements

The chronology is based on 19 AMS ^{14}C ages measured on terrestrial plant macrofossils and on ^{137}Cs measurements taken from the topmost 32 cm of the sediment record with a well-type GeLi detector following procedures detailed in Fanetti et al. (2008; Table 1 and Fig. 2a). For radiocarbon analyses, selected terrestrial macrofossils were isolated from sediment samples (thickness of 1 cm) by sieving with a 100 µm mesh under water. All radiocarbon ages were calibrated using the program Calib 6.06 (Reimer et al., 2009). All ages are reported on each master core (LL08-1 and LL08-2) according to lithological correlation (Fig. 2a). The results from radiocarbon and short-lived radio-isotope analyses were combined to produce an age-depth model for each sequence using a smooth cubic spline model available within the "Clam" software by Blaauw (2010).

3 Results

3.1 Lithological classification: laminated facies and sedimentary events

Because Lake Ledro is situated in a carbonate catchment, the autochthonous sedimentation is dominated by calcite precipitation and biogenic lake productivity (Fig. 2a), accompanied by the sedimentation of allochthonous material such as clay and organic particles. This results in a laminated and continuously deposited facies, referred to as "background" sedimentation. In detail, the background-laminated sedimentation is composed of two layers: one white carbonated and one grey clayed. The season of the biochemical calcite layer deposit is summer, whereas for the grey layer it is undetermined but could occur during winter. The solarisation (saturated and inversed colour) of core images allows to easily identify the 2 different laminae that characterise background lacustrine sedimentation in Lake Ledro, highlighting that this finely laminated facies is frequently intercalated by numerous event deposits of two different types (Fig. 2a).

The first type of sedimentary event corresponds to graded dark-brown deposits of various thicknesses (from 1 mm to 38 cm). The stratigraphic position of these intrusive event layers within the background sedimentation attests to their seasonal deposition (Mangili et al., 2005). It is impossible to determine the season of the flood layer deposit because of the relative conservation of the laminations and because the possibility of sedimentation disturbance during the flood deposit (erosive deposit) cannot be completely ruled out. If the dark-brown layer is covered by the light carbonated summer layer, we might hypothesise that the sedimentary event occurred during spring. If the dark-brown event layer is capped by the grey clayed layer, we hypothesise that it was

CPD
8, 4701–4744, 2012

Controls on the Holocene flood frequency in the Lake Ledro area

B. Vannière et al.

deposited during autumn; the great majority of our observations have this characteristic. Organic petrography observations show that organic matter included in these deposits is mainly of terrestrial origin (red amorphous organic particles; Meyers and Lallier-Vergès, 1999). Geochemical and geophysical measurements also allow us to distinguish these dark-brown layers from the background sedimentation (Fig. 2b). They are characterised by higher magnetic susceptibility values that attest to their detritic origin and by lower Ca-content, which is also in accordance with this origin. Only the Zr increase characterises the entire layer, while other detrital elements such as Si, K and Ti show an asymmetric profile and mark only the upper part of each event layer. The grading observed in these deposits is interpreted as the typical signature of hyperpycnal flood deposits in a sub-aquatic basin (Mulder and Alexander, 2001; Simonneau et al., 2012). Based on the grain-size pattern and the high content of terrestrial organic matter, these deposits are interpreted to be composed of allochthonous material, resulting from flood events in the Lake Ledro tributaries. Visual correlations between master cores LL08-1 and LL08-2 show that these layers are thicker in the proximal core LL08-2 than in the distal core LL08-1. Several hundred of these flood deposits are recorded within core LL08-1 and LL08-2 (Table 2).

In addition to these flood deposits, a second sedimentary event type can be observed as light grey-brown homogeneous deposits (Fig. 2a). The mean granulometry of these event layers is finer, and petrographic observations show that this facies is mainly composed of organic matter of lacustrine origin (grey amorphous particles; Millet et al., 2007). These are the same particles that also characterise the laminated facies, indicating their origin in the lake's biological productivity. Thus, these light grey-brown homogeneous deposits are of lacustrine origin and may correspond to subaquatic mass-movements or mass-wasting deposits (MWD) reworking and mixing lacustrine sediments from the slopes and the shores (Simonneau et al., 2012). This second type of sedimentary event is indicated by thicker layers ranging from 0.1 mm to 13 cm. This second type of event deposit is less common than the dark-brown one; 11 and 13

CPD
8, 4701–4744, 2012

deposits (up to 1.5) have been identified, respectively, in LL08-1 and LL08-2 records, while several hundred flood events deposits have been observed.

3.2 Chronology and sediment accumulation rates

Measurements of ^{137}Cs radioactivity in the upper 32 cm of core LL08-2P highlight the occurrence of 3 well-defined peaks at 29 cm, 20 cm and 6 cm (Fig. 2a). The deeper peak at 29 cm reflect the peak level of atmospheric nuclear weapons tests in the Northern Hemisphere in 1963 (Appleby, 2001), whereas the first very strong peak at 19 cm is related to the high contamination in Northern Italy induced by the Tchernobyl nuclear reactor meltdown in 1986 and previously documented within the Southern Alps in lake Como recent sediments (Fanetti et al., 2008). The upper peak at 6 cm also indicates that high contamination is very unusual. Because this high peak in ^{137}Cs reaches similar values as the one associated with the 1986 Tchernobyl accident, and because lacustrine *laminae* are tilted between 0.5 cm and 13 cm of the sediment core, this section of core LL08-2P is interpreted as a slump deposit reworking recent sediments and should therefore not be considered in the development of the age-depth model.

The results from radiocarbon dating and from the analysis of the anthropogenic radionuclide ^{137}Cs were combined to produce age-depth models for both cores using a smooth cubic spline model available within the "Clam" software (Blaauw, 2010; Fig. 3; Table 1). This model allows for the robust estimation of uncertainties and takes into account the entire probability distribution of the calibrated radiocarbon dates, avoiding any arbitrary choices. Taking into account the automatic and the naked-eye method for sedimentary event identification and counting (see next section), two age-depth models were calculated for each sequence. The average confidence interval of the error of the models is 200 yr. The mean Sediment Accumulation Rate (SAR) is higher for LL08-2 than for LL08-1, but both sequences show similar variability. The automatic method does not identify the clay cap of the sedimentary events, and thus it may underestimate the sedimentary event thickness, which explains the slight differences between the models. In general, however, the shape and slope of the curves are very similar. Considering the entire record at the scale of 10 000 yr, the sedimentary dynamics deduced from all these models appears to be relatively continuous and low ($SAR < 0.04\,mm\,yr^{-1}$ for sedimentation without sedimentary events) prior to 4000 cal BP. After this date, a long trend of increasing SAR is recorded, as are abrupt and strong increases that reach maxima at ca. 3600 1800, 1000 yr cal BP and since ca. 1850 cal AD.

3.3 Automatic and naked-eye counting of flood deposits, and frequency analysis

Core-image treatment by solarisation shows that flood deposits appear in a brown colour that is mainly characterised by the red colour in RGB scale, whereas the laminated facies is characterised by blue for the summer deposit and by the green for the clayed layer (Fig. 2a). Thus, to separate the dark-brown deposits from the background, we selected the 1/Red signal, which represents the highest amplitude over the series in RGB values (Figs. 2b and 4a). Then, we normalised the signal by removing the low-frequency trend, following the principle used for reconstruction of fire-event frequency (Long et al., 1998; Vannière et al., 2008). The low-frequency signal is estimated here by the moving first quartile with a running window of 1000 values. The normalisation corresponds to the reduced value (raw value minus the mobile quartile) divided by the mobile standard deviation: (1/Red) normalised = (((1/Red)-mobile quartile1) / mobile standard-deviation). The normalised signal contains two components: the background, which oscillates around zero, and the peak component, which is significantly different from the background. Two populations of values usually represent them: the lowest ones are interpreted as analytical noise, whereas the highest positive ones above the threshold value (TV) are assumed to express intrusive events. A Gaussian mixture model was used to decompose the peak component, i.e. to analyse the histogram plot of the peak-component frequency distribution and to choose the TV (MIXMOD Software; Biernacki et al., 2006; Fig. 4b). This model helps to disentangle two overlapping sub-distributions and to identify the upper limit of the main distribution, which may potentially be the upper limit of the analytical noise-related variation. The distribution of peaks along the sequence is evaluated by the smoothing sum of episodes with a 50 or 100-yr moving time window. The reconstruction of flood-event frequency, from cores LL08-1 and LL08-2, results from this time-series analysis of the peak components (Fig. 5). According to the lithological classification presented Sect. 3.1, naked-eye counting of the dark-brown flood deposits has been performed three times by three different persons. The results were averaged to produce a naked-eye counting value. Flood event frequency and the sum of thickness per 100 yr are presented in Fig. 5.

Results from both counting methods appear very similar if we consider the number of identified layers, the mean thicknesses or the standard deviations. Between cores LL08-1 and LL08-2, flood-event deposits are quasi-systematically thicker in core LL08-2, i.e. at the more delta-proximal location. Thus, 20 % more flood event deposits have been identified and counted in core LL08-2 compared to core LL08-1. However, the mean results obtained from both cores and methods show only thin grey-bands of uncertainty, which indicates the low amount of variability in the signals obtained from the two cores. This confirms that the reconstructed flood signal depends neither on the core location in the lacustrine basin nor on the identification/counting methods used for quantifying sedimentary event deposits.

Flood frequency appears low until 4500 cal BP, except for small increases at ca. 8000, 7500 and 7100 cal BP. Then, an abrupt increase is recorded between 4500 and 2800 cal BP, followed by a slight decrease until 1300 cal BP (650 cal AD). A new strong increase occurs after ca. 450 cal BP (1500 cal AD), reaching a maximum at ca. 150 cal BP (1800 cal AD). The bottom-left diagram of Fig. 5 shows the detailed reconstruction of flood frequency for the last 1300 yr, a period that includes the Medieval Warm Anomaly and the Little Ice Age. Seven periods of elevated flood frequency are recorded around 750, 900, 1150, 1300, 1550 and 1850 cal AD. The sum of flood thickness per 100 yr shows a similar record of flood activity except for four additional short and abrupt increases, which correspond to punctual thick flood deposits in ca. 6600, 5600, 5100 and 2700 cal BP. Mass-wasting deposits are also plotted in Fig. 5: most of the events

CPD
8, 4701–4744, 2012

are recorded during the last 4500 cal BP, only 3 events occur earlier, around 9200, 7200 and 5900 cal BP.

3.4 Background sedimentation changes

Figure 6 presents geophysical and geochemical descriptors of the whole LL08-1 sequence, including density of sediments, magnetic susceptibility and the Ca/K ratio calculated from core scanning. Calcium can be considered a proxy for autochthonous sedimentation (mainly derived from authigenic precipitation in the water column), while potassium is mainly linked to clays and may be considered a proxy for allochthonous sedimentation. The low-frequency smoothing of the data highlights the main trend of the sedimentary dynamics during the last ten millennia, i.e. the change in sediment composition associated with environmental changes, excluding sedimentary events. The Ca/K ratio that allows us to partially correct for drifts is used to track allochthonous inputs (represented by K) versus mineral autochthonous precipitation (Ca). Ca can also be detritic, as the watershed is dominated by Dolomite. Complementary calcium and zirconium elemental analyses from samples of discrete laminated facies characterise the background sedimentation.

All of these proxies show a significant change of background lacustrine sedimentation at ca. 4000. This means that, during the Bronze Age, there was an increase in GD, MS and allochthonous components (K, Zr), which indicates higher erosion in the watershed of Lake Ledro. GD, MS and Ca/K show that this high allochthonous contribution to sedimentation continues until ca. 3000–2800 cal BP. This is also indicated by the increase in SAR (Fig. 3). After this period, autochthonous sedimentation becomes dominant during the early and mid-Holocene. Around 1200–1000 cal BP (750–950 cal AD), all proxies record a new increase in detrital input into the lake (SAR, MS, Zr and Ca/K proxies), and a new period of soil erosion and land cover change begins in the catchment, lasting until the 20th century. Just a short interruption is observed in the period of ca. 1200–1400 cal BP (500–700 cal AD).

CPD
8, 4701–4744, 2012

3.5 Tree cover and pollen inferred land-use dynamics

Vegetation dynamics around the lake are documented by simplified pollen data shown in Fig. 6. Land-cover changes are in agreement and confirm the interpretation of the sedimentological analyses (Fig. 6). A first phase of landscape opening and land-use occurs between ca. 4100 and 2700 cal BP, during the Bronze Age, following by lower human pressure in the watershed until ca. 2300 cal BP. Between 2300 and 1700 cal BP, during the Roman period, human impact is perceptible but remains relatively low. Then, a new phase of decline in human activities is recorded until ca. 1200 cal BP (750 cal AD). The third phase of forest clearing and expansion of agro-pastoralism activities around the lake corresponds to the medieval period. The human impact on land crosses a new threshold and intensifies from 1000 cal AD (950 cal BP) until the 20th century, with only a short decrease around the 13th century (600 cal BP).

4 Discussion

4.1 Sedimentary event deposits and palaeoflood regime analysis

Changes in the amount, frequency and intensity of precipitation have an effect on the magnitude and timing of runoff, and thereby on the flood occurrence. Hence, long-term flood records can be used as valuable proxies of Holocene climatic variability through the analysis of variations in the temporal distribution of floods (Moreno et al., 2008). In the case of Lake Ledro, the Massangla and Pur rivers are occasionally torrential tributaries draining steep slopes. The dark-coloured flood events in the sediments record these intense hyperpycnal flood events (Mulder and Chapron, 2011).

The sedimentation of Lake Ledro offers one of the best systems to clearly detect and quantify flood deposits: the background sedimentation is dominated by autochthonous sedimentation (carbonate and lacustrine organic matter), and the flood deposits are marked by a high content of soil organic matter and appear as dark-brown layers that can be easily differentiated from the background in digital pictures. Thus, the colour data represent a more valuable proxy than geochemistry measurements, which are affected by long-term changes in the background sedimentation with the increase in terrestrial inputs since ca. 4000 cal BP (Fig. 6). Using a seismic survey to find the best undisturbed sequences and analysing two cores in a proximal and distal position in the lake guarantees the quality of our record, even though there could be some heterogeneity of deposits in the lacustrine basin (Schiefer et al., 2011).

For the hydrologist, a flood is a river-flow height or volume that exceeds some mean or average water flow state over a period of time. In contrast, the sedimentologist considers floods to be flows of sediment that exceed some threshold value, such that they induce significant solid particle input into the lake. Because there are numerous geomorphologic characteristics and sedimentological parameters, the thickness of flood deposits cannot be directly associated with the intensity of floods (Giguet-Covex et al., 2012). However, records of flood frequency are dependent on deposit thickness as a minumum thickness that defines the detectable layers, i.e. on floods that have led to the sedimentation of a minimum of allochthonous material. The methods and techniques used in this study were selected to detect the greatest portion of flood episodes that have occurred in the Ledro Lake catchment area and to provide the most exhaustive flood frequency reconstruction possible. The results show that, except for small punctuate differences, both frequency and thickness records offer the same pattern: deposit thickness increases when frequency increases, and vice-versa (Fig. 5). Only the rarest, thickest events (> 5 cm) seem to occur during periods of low or moderate flood frequency, such as those at ca. 6500, 5500, 5000, 3500, 3200, 2500 cal BP, which may reflect strong remobilisation and discharge of material stocked in the watershed during a low flooding period.

4.2 Four successive periods of palaeoenvironmental changes

Figure 6 shows that, independent of the event deposits, the background sedimentation of Lake Ledro records four main periods:

- Before 4100 cal BP, detrital flux into the lake is very low, and the vegetation around the lake is a closed forest. Pollen-inferred anthropogenic activities indicate low human impact (Joannin et al., 2012).
- After 4100 cal BP (2150 cal BC) and until 2700 cal BP (750 cal BC), environmental dynamics are marked by an increase in detrital inputs into the lake (SAR, MS, K and Zr increases) and increased pollen, indicating human activities. Meanwhile, the number of arboreal taxa decreases. This clearly indicates an increase in soil erosion, which fits with human forest clearing and the development of agro-pastoral activities. This is in agreement with the Bronze Age settlement found on the lake shores by an archaeological survey (Pinton and Carrara, 2007).
- The third period, from 2700 to 1200 cal BP (750 cal BC and 750 cal AD), encompasses the Iron Ages and the Roman and Early Medieval periods. During these periods, human activities seem relatively limited: the forest recovers and erosion strongly diminishes. Only a small increase in anthropogenic pollen (from 2300 to 1700 cal BP) indicates a human presence in the watershed that is most likely less marked by pastoralism than by crop cultivation, which in turn has a reduced effect on the forested area (Joannin et al., 2012). From 1700 to 1200 cal BP, the reduction of agro-pastoral activities may be associated with the massive migration period (Tinner et al., 2003; Büntgen et al., 2011).
- The last period of environmental change is from 1200 cal BP (750 cal AD) to the 19th century, i.e. the Middle and Modern Ages. A new increase in allochthonous input into the lake follows the opening of the forest and the expansion of human activities around the lake. This fourth period is abruptly and briefly interrupted around 700 cal BP (1350 cal AD), at the time of the European Black Death and Great Famine (Büntgen et al., 2011).

In the 19th century, the sedimentation appears strongly modified by the human control of lake-level for hydroelectricity production; consequently, the record cannot be used for palaeoenvironmental reconstruction.

CPD
8, 4701–4744, 2012

4.3 Variability in flood frequency in the early to mid-Holocene and possible orbital control

Over the last 10 000 yr, Lake Ledro's flood record shows two distinct periods, with clustering of flood events at 8000–7000 BP and after 4500–4000 cal BP (Fig. 8). In detail, the high frequency variability, i.e. above the millennial trend, notes a secular variability that appears under climatic control during the last millennium and that perfectly correlates with the Ledro lake-level reconstruction (Magny et al., 2012). Figure 8 shows similar increases in flood activity in the nearby Lake Iseo (50 km south-west of Lake Ledro; Lauterbach et al., 2012), in Southern Italy (Piccarreta et al., 2011), in the Alps (Debret et al., 2010) and in Germany (Hoffmann et al., 2008). All of these authors postulate that flooding periods are climatically driven and mainly associated with colder and moister periods, at least until 4000 to 2000 cal BP.

The three successive increases in flood frequency and lake level 8000, 7500, and 7000 cal BP appear to be the most prominent events in the early to mid Holocene at Lake Ledro. They seem synchronous with a major change in reconstructed summer temperature deviation in South-Western Europe (Fig. 8; Renssen et al., 2009). Also at this time, the Holocene SST record from marine core MD90-917 in the Adriatic Sea highlights major negative anomalies (Siani et al., 2010). This period, 8000–7000 cal BP, corresponds to the highest rate of change in annual insolation for the Holocene (Zhao et al., 2010) and a prolonged period of decrease in the residual atmospheric radiocarbon (Stuiver et al., 1998). The higher flood activity may have been driven by a combination of orbital forcing and change in solar activity. In a broad sense, these increases in flood frequency occur during periods of global cooling marked by major glacier advances in the Alps (Matthews et al., 2008). Between ca. 7000 and 4500 cal BP, Ledro's flood frequency is relatively low, except for a few very thick deposits that are synchronous with a lake-level rise around 5800–5300 cal BP. This coincides with a major worldwide cooling event (Magny et al., 2006).

CPD
8, 4701–4744, 2012

Around 4300–4000 cal BP, the ecosystems of the Alps and the Northern Mediterranean experienced a major change (the Neoglacial; Zanchetta et al., 2012), including reduced fire activity (Vannière et al., 2011), rising lake levels (Magny et al., 2009) and glacier advances (Matthews et al., 2008). Superimposed on this multicentury climate variability, the multimillennial trend of summer temperature shows a decline (Fig. 8; Renssen et al., 2009). Such a trend is in line with the precessional signal found in insolation at 60° N (Berger and Loutre, 1991): the decreased seasonal contrast of insolation reached its halfway point at this time. Synchronously, the period of flood frequency increase around 4500–4000 cal BP at Lake Ledro suggests a change in the long-term palaeohydrological regime, with a long-term repetition of period of high flood frequencies, which is also at the European scale (Fig. 8). This rupture may reflect a non-linear climate response to the orbitally driven gradual decrease in summer insolation, which controls the millennial trend toward wet conditions during the late Holocene (Mayewski et al., 2004; Zhao et al., 2010).

4.4 Variability of flood frequency during the mid- to late-Holocene and imprint of human activities

The millennial trend of Lake Ledro's flood frequency shows two marked steps changes in the rate of increase around 4500–4000 cal BP and 500 cal BP, coinciding with known global climate changes. These changes in flood dynamics are also synchronous with forest openings, soil erosion and an increase in land use in the Lake Ledro watershed; the earlier one is contemporaneous with protohistoric lake-dwelling settlements (Fig. 8; Pinton and Carrara, 2007). This suggests that at least part of the flood activity and/or the repetition of intense events, as shown by the increase of mean thickness increase of flood deposits, is linked with human activities. At the regional scale, pollen data provide strong evidence for regional anthropogenic influence, such as forest clearings and agricultural activity (Mercuri et al., 2006; Valsecchi et al., 2006). In the Western Swiss Alps, changes in Holocene vegetation are characterised by continuous landscape denudation that begins at ca. 4300 cal yr BP, with several distinct pulses of

CPD
8, 4701–4744, 2012

increasing deforestation. Each pulse can be attributed to an increase in pollen-inferred human impact and corresponds to increased landslide activity in the Lake Schwarzsee catchment area, as recorded by higher sedimentary event frequencies in the sediment record (Dapples et al., 2002).

Similarly, Macklin and Lewin (2003) reconstruct the flood frequency in Britain through the Holocene. A significant increase around 4500–4000 cal BP in their data suggests that land use has increased the sensitivity of both lowland and upland British environments. They conclude that land use plays a key role in moderating or amplifying the sensitivity to climate. A database of 506 fluvial ^{14}C ages from Germany (Fig. 8; Hoffmann et al., 2008) and comparison with palaeoclimatic and proxy data of human activities confirm that because 4500–4000 cal BP, the increased soil erosion is at least partially due to the growing population and intensive agricultural activities during the Bronze Age and cannot be unequivocally attributed to climate. Across Central and Southern Europe, studies reveal a striking synchronism in soil impacted by land use. This suggests similar land-use practices over wide areas, marked by the fire and grazing development that characterises the Bronze Age (Rius et al., 2009; Vannière et al., 2008). During this period, around the Mediterranean basin, the fire regime switches from being predominantly climate-forced to being human-driven (Vannière et al., 2010, 2011).

These observations raise the question, how were the Bronze Age populations able to transform large areas so rapidly? Although the relative contributions of climate and land use are difficult to quantify, the results obtained from Lake Ledro help to answer questions about the magnitude of ecosystem changes and about the timescales. During the period 4500–4000 yr ago, the Bronze Age population was most likely large enough to contribute to a widespread and strong increase in land erosion, but the major changes in the hydrological regime, recorded in particular by lake-level variability (Magny et al., 2012) at lake Ledro, primarily suggest orbitally driven climate change, and we postulate that the Neoglacial initiation leads to the flooding increase.

CPD
8, 4701–4744, 2012

4.5 Variability in flood frequency during the last millennium and possible solar control

To assess the main drivers of flood frequency during the last centuries and to interpret long-term changes in flood frequency, chronologies of high- and low-frequency variability were compared with independent and regional flood records and climate reconstructions (Fig. 7). The first comparison concerns the debris-flow calendar from Lago di Braies (150 km north-east of Lake Ledro; Irmler et al., 2006). Taking into account the uncertainty in the radiocarbon chronologies, both records show strong similarities in their time series. Prior to 700 cal BP (1250 cal AD), flood and debris-flow frequency is relatively low, with three slight increases at ca. 1200, 1050 and 900 cal BP (750, 900 and 1150 cal AD). A stronger increase is recorded in both records around 650 cal BP (1300 cal AD), followed by a break of a few centuries, then followed by a major increase that reaches its first maximum at ca. 400 cal BP (1550 cal AD) and a second maximum at ca. 100 cal BP (1850 cal AD). These periods of maximum flood frequency since 1500 cal AD have also been reported by Schmocker-Fackel and Naef (2010) from Northern Switzerland, and they appear to be synchronous with multiple records of Spanish flood activity (Barriendo and Rodrigo, 2006; Benito et al., 2003), suggesting that these flood patterns result from large-scale climate changes at the European scale or larger. The long-term trend of increased flood frequency during the last millennium also contains two successive periods of low and high flood frequency, which coincide with the Medieval Warm Period (MWP) followed by the cooler Little Ice Age (LIA) from ca. 1500 to 1850 cal AD. This is also in agreement with the increase in flood activity during the LIA in many Mediterranean river basins (Benito et al., 2008; Moreno et al., 2008; Wilhelm et al., 2012). The comparison with Alpine summer temperature series reconstructed from tree-ring data (Büntgen et al., 2011; Corona et al., 2011) highlights a general synchronicity between summer-temperature decreases and flood-frequency increases, such that climate appears to be the main driving factor of flood frequency variability. Finally, the comparison with the total solar irradiance record, from Beryllium-10 ice-core records (Delaygue and Bard, 2011), suggests that during the last 1300 yr, flood frequency increases occurred during all minima of solar irradiance. This timing of flood frequency increases implies that, superimposed on the local flood-producing mechanism, solar variability during the last millennium has induced a response in the hydrological regime through indirect and complex atmospheric circulation patterns (Hu et al., 2003; Mayewski et al., 2004).

The recent synthesis of seasonal characteristics of flood regimes across the Alpine–Carpathian range by Parajka et al. (2010) indicates that, in the region of Lake Ledro, the annual maximum daily precipitation is distributed between late August and November. The annual maximum flooding occurs during autumn from flood-producing storms due to southern air flows driven by the meridional southern circulation patterns. However, spring and summer floods occur before the extreme precipitation season due to increasing soil moisture from the late spring snow melt, whereas extreme events are more likely to occur as late as November. Gaume et al. (2009) also documented a marked seasonality of flash floods and in many parts of the Alpine range suggesting a mechanism involving extreme storms and southerly circulation patterns that cause warm and moist air to be advected from the Mediterranean Sea. All of these may explain the good correlation observed in Fig. 7 between Alpine summer temperature reconstruction and Lake Ledro's flood frequency variability. From the MWP into the LIA, the trend toward higher flood frequency could have resulted from the steepening of the meridional temperature gradient as the Alps cooled more rapidly than the Mediterranean. The spring flood deposits at Lake Ledro are absent during the MWP but not the LIA period (Wirth et al., 2012). These spring signals could be in agreement with the persistent positive North Atlantic Oscillation (NAO) mode that Predominated during the MWP and with the transition to more negative NAO conditions during the LIA (Trouet et al., 2009) which would have increased winter and spring precipitation on the southern slopes of the Alps and in the Northern Mediterranean regions causing flood frequency to increase during this season.

5 Conclusions

A combination of non-destructive core-scanning techniques, detailed analysis of sediment facies and AMS ^{14}C dating of terrestrial macro-remains was used to detect and characterise the Lake Ledro sediment record. Very high-resolution and continuous colour data appear to be the most relevant proxy to identify flood event deposits and to separate them from the continuous background sediments. During the early- to mid-Holocene, flood activity appears limited to short episodes of weak increases in flood frequency during periods of high lake levels, which indicate cooler and wetter climate conditions between 8000 and 7000 cal BP. After ca. 4500–4000 cal BP, flood frequency and layer thickness strongly increase synchronously with an abrupt and long-term lake-level rise at Lake Ledro. This period of flood frequency increase corresponds to a major change in hydrological regime around Lake Ledro and is in accordance with other European records of river activity, glacier extent and other proxies of climate change under global forcing factors such as insolation. The role of climate as the main forcing factor in flood activity is documented, but, since the Bronze Age and later during the Middle-Ages and modern times, forest clearing and land use, as shown with pollen and archaeological data, have strongly increased soil erosion and flood intensities, and these factors could explain the increases in the amplitude of flood activity. In lakes, allochthonous sedimentation, and in particular extreme inputs such as flood deposits, are controlled by the physiographic setting of a catchment and are moderated by climate and land-cover/land-use change.

Based on these approaches and results, our data emphasise: (1) variability of flood activity during the past 10 000 yr in the catchment area of Lake Ledro has been marked by two major changes ca. 4500–4000 cal BP and 650–450 cal BP (1300–1500 cal AD); (2) coherence between Lake Ledro's flood record and a large number of flood records available from western and Southern Europe, which document the influence of North-Atlantic climate variability on flood frequency at the southern edge of the Alps; (3) strong human impacts resulting in an increase in allochthonous inputs into the lake since the Bronze Age, which is also most likely a general phenomenon in Europe during this period of cultural change and demographic increase. Independently of the forcing factors that cause this major shift in sedimentary flux, the period ca. 4500–4000 cal BP appears to have been crucial in determining the trajectory of Western European ecosystems. Disentangling human and climate impacts on ecosystems dynamics is quite difficult because the influence of climate on societal development is not well understood, and past societal impacts on palaeoclimate change are most likely underestimated.

Acknowledgements. Financial support for this study was provided by the French ANR "LAMA" project (directed by M. Magny and N. Combourieu-Nebout, MSHE N. Ledoux, Besançon, France), and the Swiss National Science Foundation project "FloodAlp". Many thanks go to A. Stock and J. Didier for their help in conducting fieldwork and laboratory analyses.

References

Appleby, P.: Chronostratigraphic techniques in recents sediments, in: Tracking Environmental Change Using Lake Sediments. Basin Analysis, Corin, and Chronological Techniques, edited by: Last, W. and Smol, J., Kluwer Academic Publishers, Dordrecht, p. 200, 2001.

Barriendos, M. and Rodrigo, F. S.: Study of historical flood events on Spanish rivers using documentary data, Hydrol. Sci. J., 51, 765–783, 2006.

Battarbee, R. W. and Bennion, H.: Palaeolimnology and its developing role in assessing the history and extent of human impact on lake ecosystems, J. Paleolimnol., 45, 399–404, 2011.

Benito, G., Díez-Herrero, A., and de Villalta, M. F.: Magnitude and frequency of flooding in the Tagus basin (Central Spain) over the last millennium, Climate Change, 58,171–192, 2003.

Benito, G., Thorndycraft, V. R., Rico, M., Sánchez-Moya, Y., and Sopeña, A.: Palaeoflood and floodplain records from Spain: evidence for long-term climate variability and environmental changes, Geomorphology, 101, 68–77, 2008.

Berger, A. and Loutre, M. F.: Insolation values for the climate of the last 10 million years, Quaternary Sci. Rev., 10, 297–317, 1991

Beug, H. J.: Untersuchungen zur spätglazialen Vegetationsgeschichte im Gardaseegebiet unter besonderer Berücksichtigung der mediterranen Arten, Flora, 154, 401–444, 1964.

Beug, H. J.: Leitfaden der Pollenbestimmung für Mitteleuropa und angrenzende Gebeite, Pfeil, München, 542 pp., 2004.
Biernacki, C., Celeux, A., Govaert, G., and Langrognet, F.: Model-based cluster and discriminant analysis with the MIXMOD software, Comput. Stat. Data Anal., 51/52, 587–600, 2006.
Blaauw, M.: Methods and code for "classical" age-modelling of radiocarbon sequences, Quaternary Geochronol., 5, 512–518, 2010.
Büntgen, U., Tegel, W., Nicolussi, K., McCormick, M., Frank, D., Trouet, V., Kaplan, J. O., Herzig, F., Heussner, K. U., Wanner, H., Luterbacher, J., and Esper, J.: 2500 years of European climate variability and human susceptibility, Science, 331, 578–582, doi:10.1126/science.1197175, 2011.
Chapron, E., Arnaud, F., Noël, H., Revel, M., Desmet, M., and Perdereau, L.: Rhone River flood deposits in Lake Le Bourget: a proxy for Holocene environmental changes in the NW Alps, France, Boreas, 34, 404–416, 2005.
Corona, C., Edouard, J.-L., Guibal, F., Guiot, J., Bernard, S., Thomas, A., and Denelle, N.: Long-term summer (AD751–2008) temperature fluctuation in the French Alps based on tree-ring data, Boreas, 40, 351–366, 2011.
Coulthard, J. C. and Macklin, M. G.: How sensitive are river systems to climate and land-use changes? A model based evaluation, J. Quaternary Sci., 16, 347–351, 2001.
Dapples, F., van Leeuwen, A. F., van der Knaap, J. F. N., Dimitriadis, S., and Oswald, D.: Paleolimnological evidence for increased landslide activity due to forest clearing and land-use since 3600 cal BP in the Western Swiss Alps, J. Paleolimnol., 27, 239–248, 2002.
Dearing, J. A. and Jones, R. T.: Coupling temporal and spatial dimensions of global sediment flux through lake and marine sediment records, Global Planet. Change, 39, 147–168, 2003.
Dearing, J. A., Battarbee, R. W., Dikau, R., Larocque, I., and Oldfield, F.: Human-environment interactions: learning from the past, Regio. Environ. Change, 6, 1–16, 2006.
Debret, M., Chapron, E., Desmet, M., Rolland-Revel, M., Magand, O., Trentesaux, A., Bout-Roumazeille, V., Nomade, J., and Arnaud, F.: North Western Alps Holocene paleohydrology recorded by flooding activity in Lake Le Bourget, France, Quaternary Sci. Rev., 29, 2185–2200, 2010.
Delaygue, G. and Bard, E.: An Antarctic view of Beryllium-10 and solar activity for the past millennium, Clim. Dynam., 36, 2201–2218, 2011.
Gaume, E., Bain, V., Bernardara, P., Newinger, O., Barbuc, M., Bateman, A., Blaškovicǒvá, L., Blöschl, G., Borga, M., Dumitrescu, A., Daliakopoulos, I., Garcia, J., Irimescu, A.,

Kohnova, S., Koutroulis, A., Marchi, L., Matreata, S., Medina, V., Preciso, E., Sempere-Torres, D., Stancalie, G., Szolgay, J., Tsanis, I., Velasco, D., and Viglione, A.: A compilation of data on European flash floods, J. Hydrol., 367, 70–78, 2009.
Giguet-Covex, C., Arnaud, F., Poulenard, J., Disnar, J. R., Delhon, C., Francus, P., David, F., Enters, D., Rey, P. J., and Delannoy, J. J.: Changes in erosion patterns during the Holocene in a currently treeless subalpine catchment inferred from lake sediment geochemistry (Lake Anterne, 2063 m asl, NW French Alps): the role of climate and human activities, Holocene, 21, 651–665, 2011.
Gilli, A., Anselmetti, F. S., Glur, L., and Wirth, S. B.: Lake sediments as archives of reccurrence rates and intensities of past flood events, in: Dating Torrential Processes on Fans and Cones – Methods and Their Application for Hazard and Risk Assessment, edited by: Michelle Schneuwly-Bollschweiler, M. S., Stoffel, M., and Rudolf-Miklau, F., Advances in Global Change Research, 47, Springer, The Netherlands, Dordrecht, 2012.
Gobet, E., Tinner, W., Hochuli, P., van Leeuwen, J., and Ammann, B.: Middle to Late Holocene vegetation history of the Upper Engadine (Swiss Alps): the role of man and fire, Veg. Hist. Archaeobot., 12, 143–163, 2003.
Gunn, D. E. and Best, A. I.: A new automated non-destructive system for high resolution multi-sensor core logging of open sediment cores, Geo-Marine Lett., 18, 70–77, 1998.
Hoffmann, T., Lang, A., and Dikau, R.: Holocene river activity: analysing 14C-dated fluvial and colluvial sediments from Germany, Quaternary Sci. Rev., 27, 2031–2040, 2008.
Hoffmann, T., Erkens, G., Gerlach, R., Klostermann, J., and Lang, A.: Trends of controls of Holocene floodplain sedimentation in the Rhine catchment, Catena, 77, 96–106, 2010.
Fanetti, D., Anselmetti, F. S., Chapron, E., Sturm, M., and Vezzoli, L.: Megaturbidite deposits in the Holocene basin fill of Lake Como (Southern Alps, Italy), Palaeogeogr. Palaeocl., 259, 323–340, 2008.
Feng Sheng Hu, F. S., Kaufman, D., Yoneji, S., Nelson, D., Shemesh, A., Huang, Y., Tian, J., Bond, G., Clegg, B., and Brown, T.: Cyclic variation and solar forcing of holocene climate in the Alaskan subarctic, Science, 301, 1890–1893, 2003.
Irmler, R., Daut, G., and Mäusbacher, R.: A debris flow calendar derived from sediments of lake Lago di Braies (N. Italy), Geomorphology, 77, 69–78, 2006.
Joannin, S., Vannière, B., Galop, D., Peyron, O., Haas, J. N., Magny, M., Gilli, A., Chapron, E., Wirth, S., Anselmetti, F., and Desmet, M.: Climate and vegetation changes along Lateglacial

and early-mid Holocene in Lake Ledro (Southern Alps, Italy), Clim. Past Discuss., in preparation, 2012.

Knox, J. C.: Sensitivity of modern and Holocene floods to climate change, Quaternary Sci. Rev., 19, 439–457, 2000.

Lauterbach, S., Chapron, E., Brauer, A., Hüls, M., Gilli, A., Arnaud, F., Piccin, A., Nomade, J., Desmet, M., and von Grafenstein, U.: A sedimentary record of Holocene surface runoff events and earthquake activity from Lake Iseo (Southern Alps, Italy), The Holocene, 22, 749–760, 2012.

Lenton, T. M., Held, H., Kriegler, E., Hall, J. W., Lucht, W., Rahmstorf, S., and Schellnhuber, H. J.: Tipping elements in the Earth's climate system, Proc. Natl. Acad. Sci., 105, 1786–1793, 2008

Long, C. J., Whitlock, C., Bartlein, P. J., and Millspaugh, S. H.: A 9000-year fire history from the Oregon Coast Range, based on a high-resolution charcoal study, Can. J. Forest Res., 28, 774–787, 1998.

Macklin, M. G. and Lewin, J.: River sediments, great floods and centennial-scale Holocene climate change, J. Quaternary Sci., 18, 101–105, 2003.

Macklin, M. G., Benito, G., Gregory, K. J., Johnstone, E., Lewin, J., Michczynska, D. J., Soja, R., Starkel, L., and Thorndycraft, V. R.: Past hydrological events reflected in the Holocene fluvial record of Europe, Catena, 66, 145–154, 2006.

Magny, M., Leuzinger, U., Bortenschlager, S., and Haas, J. N.: Tripartite climate reversal in Central Europe 5600–5300 years ago, Quaternary Res., 65, 3–19, 2006.

Magny, M., Vannière, B., Zanchetta, G., Fouache, E., Touchais, G., Petrika, L., Coussot, C., Walter-Simonnet, A. V., and Arnaud, F.: Possible complexity of the climatic event around 4300–3800 cal. BP in the central and Western Mediterranean, The Holocene, 19, 1–11, 2009.

Magny, M., Vannière, B., Calo, C., Millet, L., Leroux, A., Peyron, O., Zanchetta, G., La Mantia, T., and Tinner, W.: Holocene hydrological changes in South-Western Mediterranean as recorded by lake-level fluctuations at Lago Preola, a coastal lake in Southern Sicily, Italy, Quaternary Sci. Rev., 30, 2459–2475, 2011.

Magny, M., Joannin, S., Galop, D., Vannière, B., Haas, J. N., Basseti, M., Bellintani, P., Scandolari, R., and Desmet, M.: Holocene paleohydrological changes in the Northern Mediterranean borderlands as reflected by the lake-level record of Lake Ledro, North-Eastern Italy, Quaternary Res., 77, 382–396, 2012.

Mangili, C., Brauer, A., Moscariello, A., and Naumann, R.: Microfacies of detrital event layers deposited in Quaternary varved lake sediments of the Piànico-Sèllere Basin (Northern Italy), Sedimentology, 52, 927–943, 2005.

Matthews, J. A. and Dresser, P. Q.: Holocene glavcier varaition chronology of the Smørstabbtindan massif, Jotunheimen, Southern Norway, and the recognition of Century-to millenial-scale European Neoglacial Events, The Holocene, 18, 181–201, 2008.

Mayewski, P. A., Rohling, E., Stager, C., Karlén, W., Maasch, K. A., Meeker, L. D., Meyerson, E., Gasse, F., van Kreveld, S., Holmgren, K., Lee-Thorp, J., Rosqvist, G., Rack, F., Staubwasser, M., and Schneider, R.: Holocene climate variability, Quaternary Res., 62, 243–255, 2004.

Mercuri, A. M., Accorsi, C. A., Mazzanti, M. B., Bosi, G., Cardarelli, A., Labate, D., Marchesini, M., and Grandi, G. T.: Economy and environment of Bronze Age settlements – Terramaras – on the Po Plain (Northern Italy): first results from the archaeobotanical research at the Terramara di Montale, Veg. Hist. Archaeobot., 16, 43–60, 2006.

Meyers, P. and Lallier-Vergès, E.: Lacustrine sedimentary organic matter records of Late Quaternary paleoclimates, J. Paleolimnol., 21, 345–372, 1999.

Millet, L., Vannière, B., Verneaux, V., Mangy, M., Disnar, J. R., Laggoun-Défarge, F., Walter-Simonnet, A. V., Bossuet, G., Ortu, E., and de Beaulieu, J. L.: Response of littoral chironomid communities and organic matter to late glacial lake-level, vegetation and climate changes at Lago dell'Accesa (Tuscany, Italy), J. Paleolimnol., 38, 525–539, 2007.

Moore, P. D., Webb, J. A., and Collinson, M. E.: Pollen Analysis, Blackwell Scientific Publications, London, 1991.

Moreno, A., Valero-Garcés, B. L., Gonzales-Sampériz, P., and Rico, M.: Flood response to rainfall variability during the last 2000 years inferred from the Taravilla Lake record (Central Iberian Range, Spain), J. Paleolimnol., 40, 943–961, 2008.

Mulder, T. and Alexander, J.: The physical character of subaqueous sedimentary density flows and their deposits, Sedimentology, 48, 269–299, 2001.

Mulder, T. and Chapron, E.: Flood deposits in continental and marine environments: character and significance, in: Sediment Transfer from Shelf to Deep Water – Revisiting the Delivery System, edited by: Slatt, R. M. and Zavala, C., AAPG Stud. Geol., 61, 1–30, 2011.

Parajka, J., Kohnova, S., Balint, G., Barbuc, M., Borga, M., Claps, P., Cheval, S., Gaume, E., Hlavcova, K., Merz, R., Pfaundler, M., Stancalie, G., Szolgay, J., and Bloschl, G.: Seasonal

characteristics of flood regimes across the Alpine-Carpathian range, J. Hydrol., 394, 78–89, 2010.
Piccarreta, M., Caldara, M., Capolongo, D., and Boenzi, F.: Holocene geomorphic activity related to climatic change and human impact in Basilicata, Southern Italy, Geomorphology, 128, 137–147, 2011.
Pinton, V. and Carrara, N.: La collezione della palafitta di Ledro del Museo di Antropologia dell'Università di Padova: ricostruzione del paleoambiente, Annali dell'Università degli Studi di Ferrara – Museologia Scientifica e Naturalistica, Special Volume, 11–14, 2007.
Reille, M.: Pollen et spores d'Europe et d'Afrique du nord. Laboratoire de Botanique Historique et Palynologie, Université d'Aix-Marseille, France, 1992–1998.
Reimer, P. J., Baillie, M. G. L., Bard, E., Bayliss, A., Beck, J. W., Blackwell, P. G., Bronk , Buck, C. E., Burr, G. S., Edwards, R. L., Friedrich, M., Grootes, P. M., Guilderson, T. P., Hajdas, I., Heaton, T. J., Hogg, A. G., Hughen, K. A., Kaiser, K. F., Kromer, B., McCormac, F. G., Manning, S. W., Reimer, R. W., Richards, D. A., Southon, J. R., Talamo, S., Turney, C. S. M., van der Plicht, J., Weyhenmeyer, C. E.: IntCal09 and Marine09 radiocarbon age calibration curves, 0–50 000 years cal BP, Radiocarbon, 51, 1111–1150, 2009.
Renssen, H., Seppä, H., Heiri, O., Roche, D. M., Goosse, H., and Fichefet, T.: The spatial and temporal complexity of the Holocene thermal maximum, Nat. Geosci., 2, 411–414, 2009.
Rius, D., Vannière, B., and Galop, D.: Fire frequency and landscape management in the Northwestern Pyrenean piedmont, France, since the early Neolithic (8000 cal. BP), The Holocene, 19, 847–859, 2009.
Ruddiman, W. F.: The anthropogenic greenhouse era began thousands of years ago, Climatic Change, 61, 261–293, 2003.
Ruddiman, W. F.: The early anthropogenic hypothesis: challenges and responses, Rev. Geophys., 45, RG4001, doi:10.1029/2006RG000207, 2007.
Schiefer, E., Gilbert, R., and Hassan, M.: A lake sediment-based proxy of floods in the Rocky Mountain Front Ranges, Canada, J. Paleolimnol., 45, 137–149, 2011.
Schmocker-Fackel, P. and Naef, F.: Changes in flood frequencies in Switzerland since 1500, Hydrol. Earth Syst. Sci., 14, 1581–1594, doi:10.5194/hess-14-1581-2010, 2010.
Siani, G., Paterne, M., and Colin, C.: Late Glacial to Holocene planktic foraminifera bioevents and climatic record in the South Adriatic Sea, J. Quaternary Sci., 25, 808–821, doi:10.1002/jqs.1360, 2010.

CPD
8, 4701–4744, 2012

Simonneau, A., Chapron, E., Vanníere, B., Wirth, S. B., Gilli, A., Di Giovanni, C., Anselmetti, F. S., Desmet, M., and Magny, M.: Multidisciplinary distinction of mass-movement and flood-induced deposits in lacustrine environments: implications for Holocene palaeohydrology and natural hazards (Lake Ledro, Southern Alps, Italy), Clim. Past Discuss., 8, 3205–3249, doi:10.5194/cpd-8-3205-2012, 2012.
Støren, E. N., Dahl, S. O., Nesje, A., and Paasche, Ø.: Identifying the sedimentary imprint of high-frequency Holocene river floods in lake sediments: development and application of a new method, Quaternary Sci. Rev., 29, 3021–3033, 2010.
Stuiver, M., Reimer, P. J., Bard, E., Beck, J. W., Burr, G. S., Hughen, K. A., Kromer, B., McCormac, G., van der Plicht, J., and Spurk, M.: Intcal98 radiocarbon age calibration, 24 000–0 cal BP, Radiocarbon, 40, 1041–1083, 1998.
Tinner, W., Lotter, A. F., Ammann, B., Conedera, M., Hubschmid, P., van Leeuwen, J. F. N., and Wehrli, M.: Climatic change and contemporaneous land-use phases north and south of the Alps 2300 BC to 800 AD, Quaternary Sci. Rev., 22, 1447–1460, 2003.
Trouet, V., Esper, J., Graham, N. E., Baker, A., Scourse, J. D., and Frank, D. C.: Persistent positive North Atlantic Oscillation mode dominated the Medieval Climate Anomaly, Science, 324, 5923, doi:10.1126/science.1166349, 2009.
Valsecchi, V., Tinner, W., Finsinger, W., and Ammann, B.: Human impact during the Bronze Age on the vegetation at Lago Lucone (Northern Italy), Veg. Hist. Archaeobot., 15, 99–113, 2006.
Vannière, B., Bossuet, G., Walter-Simonnet, A.-V., Ruffaldi, P., Adatte, T., Rossy, M., and Magny, M.: High resolution record of environnemental changes and tephrochronological markers of the Last Glacial-Holocene Transition at Lake Lautrey (Jura, France), J. Quaternary Sci., 18, 797–808, 2004.
Vannière, B., Colombaroli, D., Chapron, E., Leroux, A., Tinner, W., and Magny, M.: Climate versus human-driven fire regimes in Mediterranean landscapes: the Holocene record of Lago dell'Accesa (Tuscany, Italy), Quaternary Sci. Rev., 27, 1181–1196, 2008.
Vannière, B., Colombaroli, D., and Roberts, N.: A fire paradox in ecosystems around the Mediterranean, PAGES News, 18, 2, 63–65, 2010.
Colombaroli, D., Daniau, A. L., Finsinger, W., Gil-Romera, G., Kaltenrieder, P., Pini, R., Sadori, L., Turner, R., Valsecchi, V., and Vescovi, E.: Circum-Mediterranean fire activity and climate changes during the mid Holocene environmental transition (8500–2500 cal yr BP), The Holocene 21, 1, 53–73, 2011.

CPD
8, 4701–4744, 2012

Controls on the Holocene flood frequency in the Lake Ledro area

B. Vannière et al.

Vasskog, K., Nesje, A., Støren, E. N., Waldmann, N., Chapron, E., and Ariztegui, D.: A Holocene record of snow-avalanche and flood activity reconstructed from a lacustrine sedimentary sequence in Oldevatnet, Western Norway, The Holocene, 21, 597–614, 2011.
Wilhelm, B., Arnaud, F., Sabatier, P., Crouzet, C., Brisset, E., Chaumillon, E., Disnar, J.-R., Guiter, F., Malet, E., Reyss, J.-L., Tachikawa, K., Bard, E., and Delannoy, J.-J.: 1400 years of extreme precipitation patterns over the Mediterranean French Alps and possible forcing mechanisms, Quaternary Res., 78, 1–12, doi:10.1016/j.yqres.2012.03.003, 2012.
Wirth, S. B., Gilli, A., Glur, L., Anselmetti, F. S., Ariztegui, D., Simonneau, A., Chapron, E., Vannière, B., and Magny, M.: Reconstructing the seasonality of late Holocene flood events using varved lake sediments of Lake Ledro (Southern Alps, Italy), 3rd PAGES Varves, Working Group Workshop, Manderscheid, Germany, 2012.
Zanchetta, G., Giraudi, C., Sulpizio, R., Magny, M., Drysdale, R. N., and Sadori, L.: Constraining the onset of the Holocene "Neoglacial" over the central Italy using tephra layers, Quaternary Res., 78, 236–247, doi:10.1016/j.yqres.2012.05.010, 2012.
Zhao, C., Yu, Z., and Zhao, Y.: Holocene climate trend, variability, and shift documented by lacustrine stable-isotope record in the Northeastern United States, Quaternary Sci. Rev., 29, 1831–1843, 2010.
Zolitschka, B., Behre, K.-E., and Schneider, J.: Human and climatic impact on the environment as derived from colluvial, fluvial and lacustrine archives – examples from the Bronze Age to the Migration period, Germany, Quaternary Sci. Rev., 22, 81–100, 2003.

Table 1. Radiocarbon and ^{137}Cs ages of cores LL08-1 and LL08-2, with the correlations between them.

Radiocarbon age core LL080-1 (1 cm thick sample)				Correlation with core LL08-2			^{14}C Age	Calibrated age*	Material
Lab. code	Sect° Name	Sect° Depth	MC Depth	Sect° Name	Sect° Depth	MC Depth	BP	2s cal BP	
POZ-27888**	P1a (P2)	21 (30)	16.5	LL082-P	38.5	21.7	255 ± 30	−4–430	Wood-Peat-Charcoal
POZ-30216	P1b	17	82.2	LL082-P	113.5	96.7	290 ± 30	288–458	Wood-Peat-Charcoal
POZ-30218	P1b	77	142.2	LL082-A1a	53.5	190.7	1020 ± 30	802–1048	Wood-Peat-Charcoal
POZ-30219	A2a	68	193.8	LL082-A1a	148	285.2	1445 ± 30	1297–1386	Wood-Peat-Charcoal
POZ-30220	A2a	113	238.8	LL082-A1 b	40.5	335.1	1945 ± 30	1823–1970	Wood-Peat-Charcoal
POZ-30221	A3a	36	298.8	LL082-B1a	17.5	443.1	2520 ± 35	2487–2743	Wood-Peat-Charcoal
POZ-27890	A3a	88	350.8	LL082-B1a	112	537.6	3095 ± 30	3244–3383	Wood-Peat-Charcoal
POZ-30222	B2a	21	402.6	LL082-B1b	46.5	626	3030 ± 35	3082–3354	Wood-Peat-Charcoal
POZ-27891	B2a	80	461.6	LL082-A2a	40	713.3	4080 ± 35	4441–4810	Wood-Peat-Charcoal
POZ-30223	A3b	91	499.2	LL082-A2a	91	764.3	4550 ± 35	5051–5319	Wood-Peat-Charcoal
POZ-27892	B2b	20	562.4	LL082-A2b	73	896.9	5720 ± 40	6412–6634	Wood-Peat-Charcoal
POZ-30224	A4a	46	616	LL082-B2a	54	1011.3	7270 ± 50	7981–8180	Wood-Peat-Charcoal
POZ-27894	A4a (B2b)	71.5 (109)	641.5	LL082-B2a	104.5	1061.8	8385 ± 35	9303–9486	Wood-Peat-Charcoal
Radiocarbon age core LL080-2 (1 cm thick sample)				Correlation with core LL08-1			^{14}C Age	Calibrated age*	Material
ETH-39232	A1b	8.5	303.1	A2a	84.5	210.5	1765 ± 35	1569–1812	leaf remains
ETH-40410	B1a	68	493.6	A3a	65	328.1	2890 ± 50	2876–3208	leaf remains
ETH-40411	B1b	86.5	666	B2a	43	424.9	3575 ± 35	3728–3978	leaf remains
ETH-39233	A2b	16	839.9	A3b	127	535.8	5200 ± 35	5902–6170	leaf remains and needles
ETH-39234	A2b	136.5	960.4	A4a	19	589	6530 ± 40	7330–7558	needles
ETH-39235	B2a	108	1065.3	A4a	73	643	8405 ± 40	9306–9521	needles
^{137}Cs age core LL080-2 (0.5 cm thick sample)				Correlation with core LL08-1			^{137}Cs Age		
^{137}Cs86d	P	10.25					1986 doubling		sediment bulk
^{137}Cs86	P	23.25	6.45	P1a	8.75	4.55	1986 real	−37–−35	sediment bulk
^{137}Cs63	P	31.25	14.45	P1a	15.5	11.3	1963	−14–−12	sediment bulk

* Calibrated with Calib 6.0 (Reimer et al., 2009).
** Age rejected.

Table 2. Descriptive statistics of flood deposits from both cores and methods.

	Core 08-1		Core 08-2	
Counting method	Automatic	Naked-eye	Automatic	Naked-eye
Number of deposits	387	408	507	482
Sum of thickness (cm)	206.1	219.8	378.1	419.8
Minimum of thickness (mm)	0.3	1	0.3	1
Maximum of thickness	15.8	16.0	37.5	38.0
Mean of thickness	0.53	0.54	0.75	0.87
Median of thickness	0.13	0.20	0.15	0.20
First quartile of thickness	0.06	0.10	0.06	0.10
Third quartile of thickness	0.41	0.40	0.42	0.50
Standard deviation	1.32	1.33	2.45	2.60

CPD
8, 4701–4744, 2012

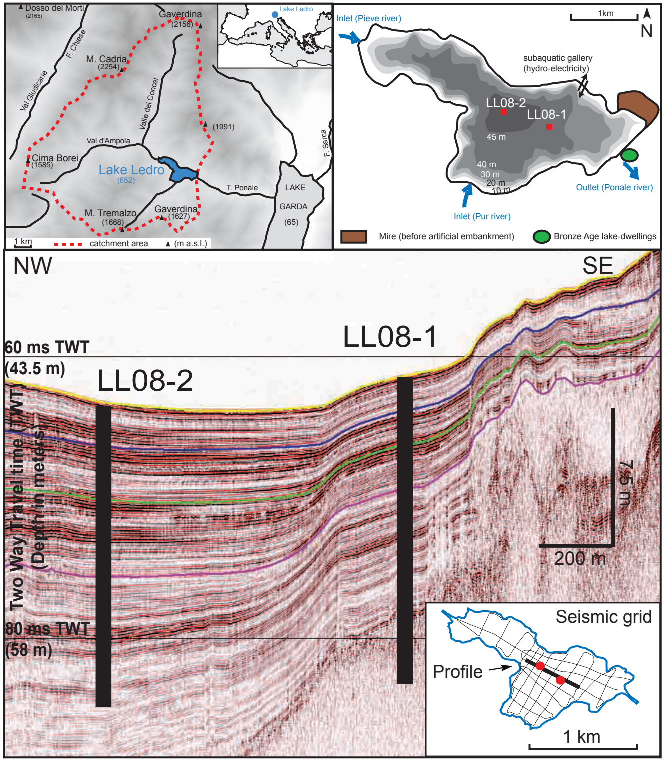

Fig. 1. Location of Lake Ledro (Trentino, Italy) and its catchment (top-left panel); the bathymetry of the lake and positions of the coring sites, inlets, outlet and archaeological site (top-right panel); a NW-SE seismic profile, with positions of cores LL08-2 and LL08-1 (bottom panel).

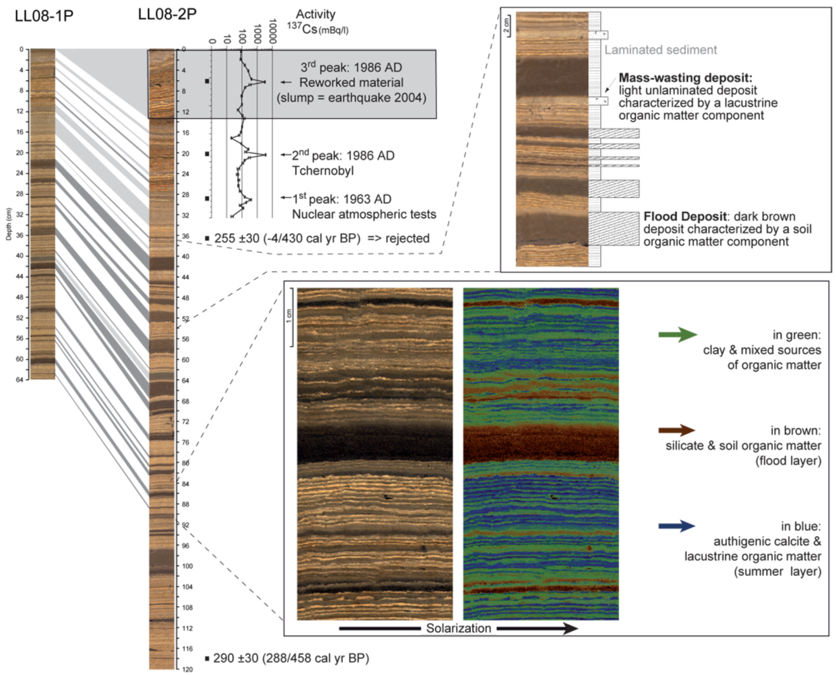

Fig. 2a. Scans, ^{137}Cs measurements and radiocarbon dates from gravity cores (1P and 2P) sampled at sites of cores LL08-1 and LL08-2. Visual inspection of the cores from Lake Ledro shows a laminated yellow-grey sediment (background sediment) interspersed with fine-grained brown units that are usually rich in terrestrial organic matter corresponding to allochthonous event layers or flood deposits (FD; bottom zoom-box). Unlaminated mass-wasting deposits (MWD) were also identified and could be easily distinguished from FD by their light colour and their lacustrine organic component (top zoom-box). All of these deposits are considered to be instantaneous and were removed from the age-depth models (Fig. 4). Solarisation is an effect used in photography that causes an image recorded on a negative to be reversed in tone.

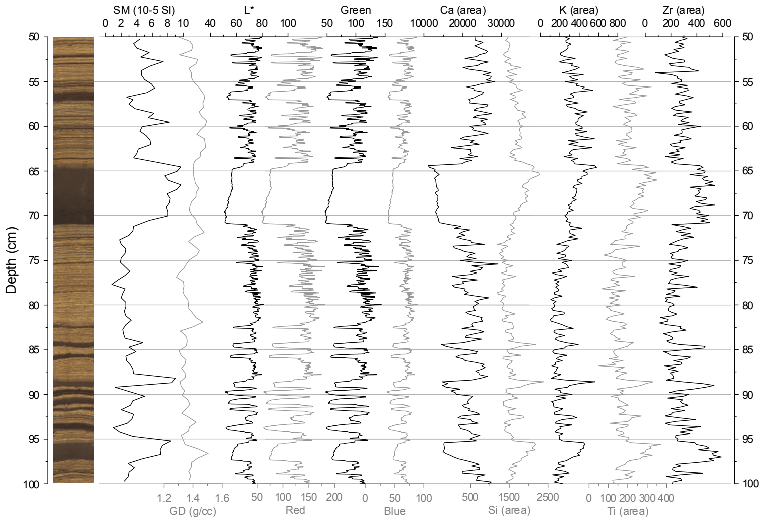

Fig. 2b. Scans, Magnetic Susceptibility (MS) and Gamma Density (GD) measurements, CIE_L* and RGB colour data, and main elements from XRF measurements of a 50 cm long section from core LL08-1. Flood deposits are characterised by higher MS and Zr values and by lower L*, RGB and Ca values than the background sedimentation. There is no clear variation in GD. Si, K and Ti values increase from the base to the top of the layers within the brown flood deposits. These reflect the fining-up of the majority of these layers by coarse silt material at the base and silty clay on the top. Their dark colour is due to a high content of organic matter that is reworked from soils.

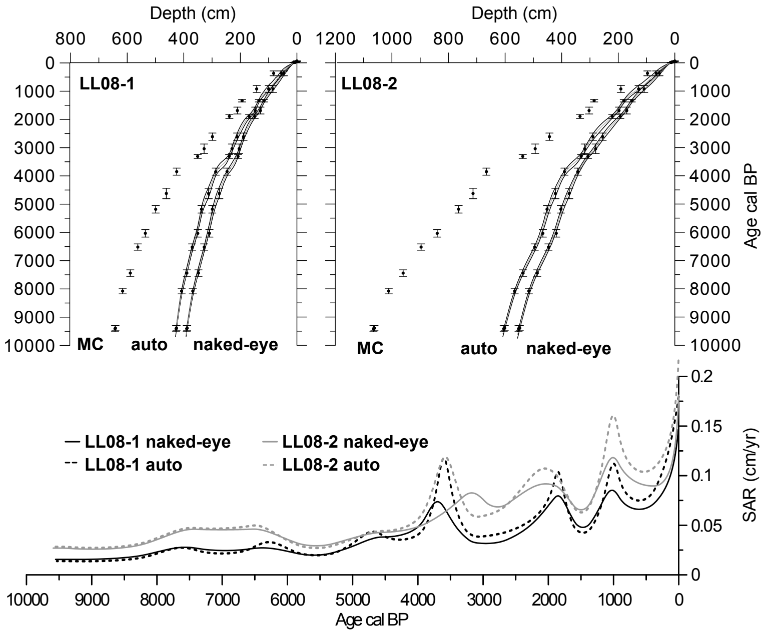

Fig. 3. Age/depth models and respective Sediment Accumulation Rate (SAR) from cores LL08-1 and LL08-2. MC: master core; auto: without automatic count of flood deposits and naked-eye mass-wasting deposits; naked-eye: without naked-eye count of sedimentary events (flood deposits and mass-wasting deposits).

CPD
8, 4701–4744, 2012
Controls on the Holocene flood frequency in the Lake Ledro area
B. Vannière et al.

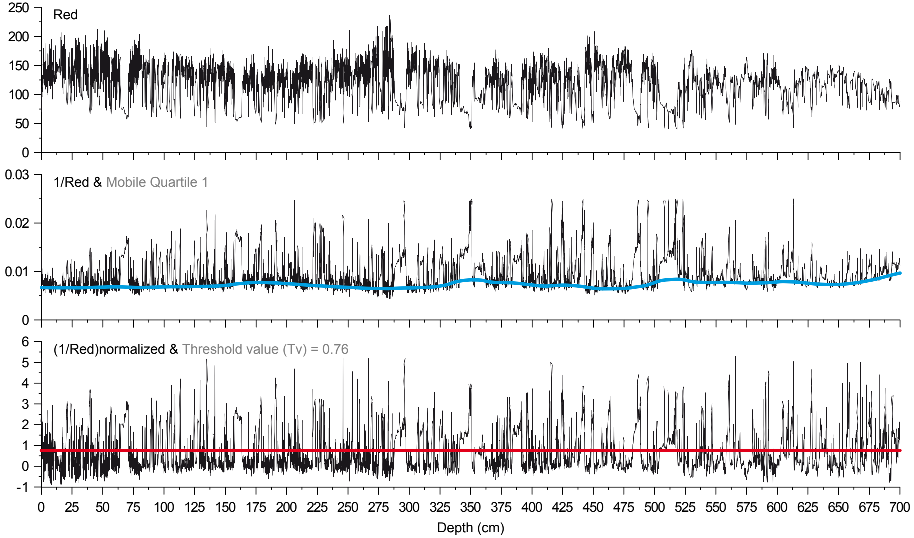

Fig. 4a. Raw and normalised red colour data from core LL08-1, and the threshold value detected with the Gaussian mixture model (Fig. 3b). (1/Red) normalised = (((1/red)-mobile quartile1)/Mobile standard-deviation); the running window is 1000 values.

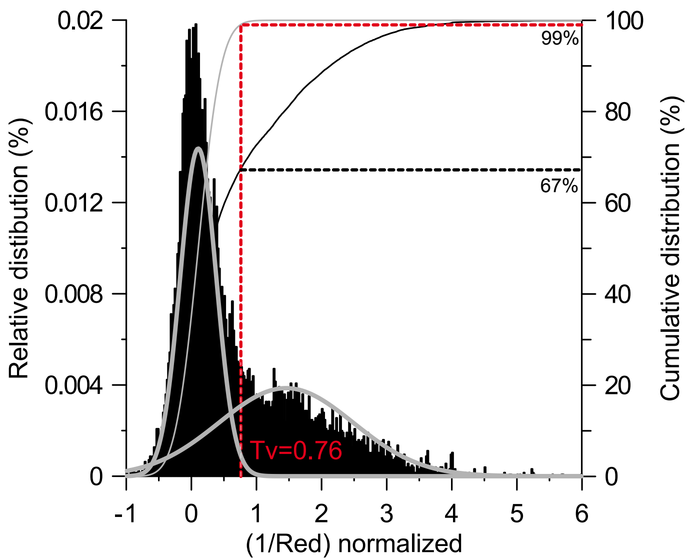

Fig. 4b. Gaussian mixture model of the normalised red colour data (Fig. 3a) used to disentangle two overlapping sub-distributions and to identify the upper limit of the main distribution (threshold value).

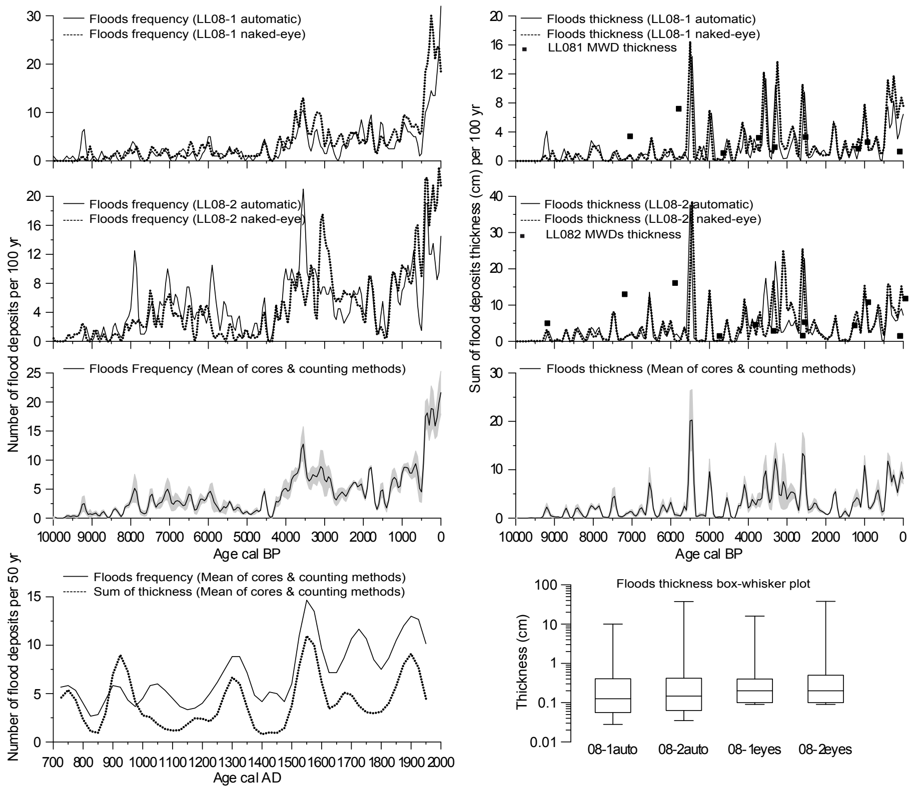

Fig. 5. Flood frequency and thickness sum per 100 yr for both cores (LL08-1 and LL08-2) and from both naked-eye and automatic counting methods; thickness of mass-wasting deposits from both cores; average curves from the four inferred records and their descriptive statistics are presented in the bottom-left diagram and in Table 2, respectively. A magnified view of detailed flood frequency (events per 50 yr) covering the last 1300 yr is plotted at the bottom-left of the figure.

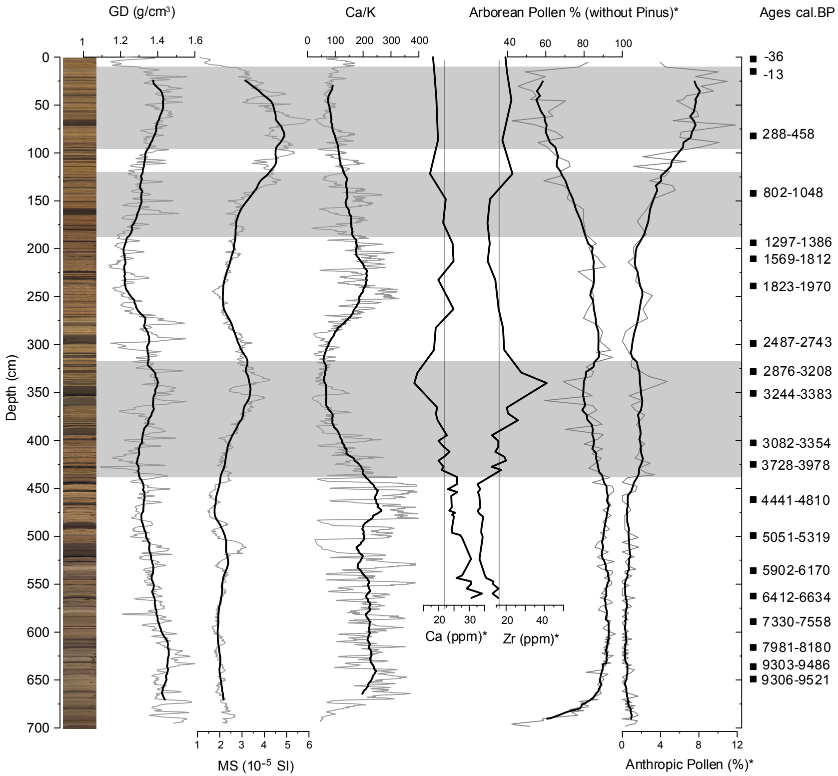

Fig. 6. Geophysical and geochemical proxies from the entire master core LL08-1, with calibrated radiocarbon ages. *Pollen analyses: Zr and Ca ICP-AES concentration measurements have been made on background sedimentation only. The Ca/K ratio is calculated from XRF measurements from the entire master core, as well as Gamma Density (GD) and Magnetic Susceptibility (MS) data.

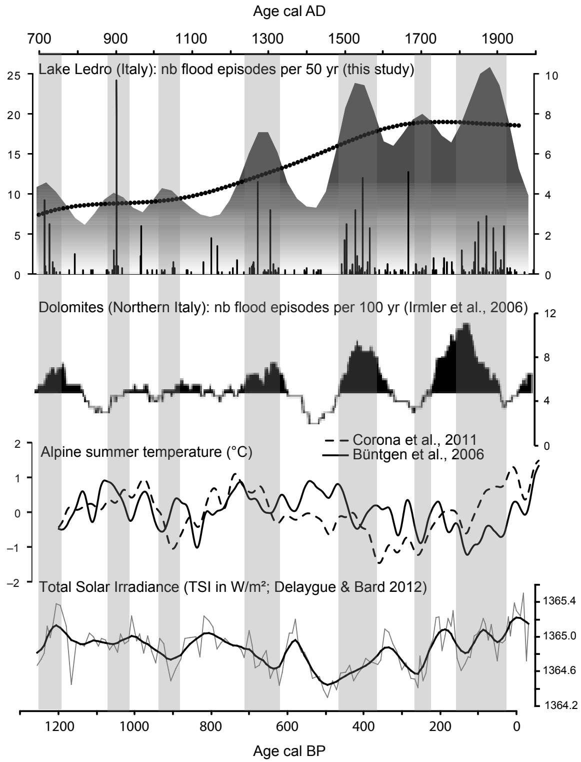

Fig. 7. Lake Ledro's flood frequency for the last 1300 yr, compared with debris flow records from Lago di Braies (Dolomite Alps), 150 km NE from Lake Ledro (Irmler et al., 2006), with Alpine temperatures reconstructed from tree-ring studies (Büntgen et al., 2006; Corona et al., 2011) and with total solar insolation reconstructed from ^{10}Be records (Delaygue and Bard, 2012).

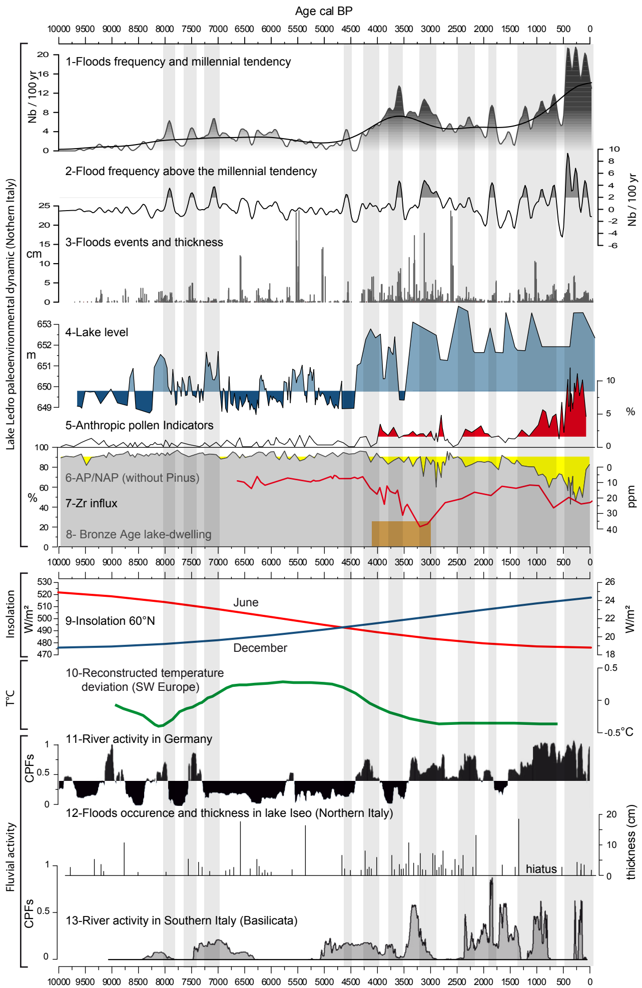

CPD
8, 4701–4744, 2012

Fig. 8. Lake Ledro's results compared with other regional and continental records of climate and environmental changes. 1 – flood-deposit frequency, with the millennial trend; 2 – submillennial flood deposit frequency, i.e. above the millennial trend (dashed: 2 times greater); 3 – flood events and thicknesses (1 to 3: Lake Ledro deep cores LL08-1 and 2; this study); 4 – Lake Ledro lake levels (littoral cores; Magny et al., 2012); 5 – anthropogenic pollen (see text for the list of taxa); 6 – arboreal pollen (5 and 6: Ledro deep core LL08-1; Joannin et al., 2012); 7 – Zr ICP-AES concentration (Ledro deep core LL08-1); 8 – chronology of the Bronze Age lake dwellings (see location on Fig. 1; Pinton and Carrara, 2007); 9 – June and December insolation at 60° N (Berger and Loutre, 1991); 10 – reconstructed deviation of summer temperatures from pollen data for SW Europe (Renssen et al., 2009); 11 – cumulative probability density functions of ^{14}C dates associated with major floods in Germany (Hoffmann et al., 2008); 12 – flood events and thicknesses from Lake Iseo (50 km SW from Lake Ledro; Lauterbach et al., 2012); 13 – cumulative probability density functions of ^{14}C dates associated with major flooding in Basilicata, Southern Italy (Piccarreta et al., 2011).

CPD
8, 4701–4744, 2012